The American Journal of Pathology, Vol. 174, No. 6, June 2009

DOI: 10.2353/ajpath.2009.081012

Neurobiology

Accelerated Course of Experimental Autoimmune Encephalomyelitis in PD-1-Deficient Central Nervous System Myelin Mutants

Antje Kroner,*† Nicholas Schwab,*‡ Chi Wang Ip,*† Sonja Ortler,*‡ Kerstin Göbel,*‡ Klaus-Armin Nave,§ Mathias Mäurer,*† Rudolf Martini,*† and Heinz Wiendl*‡

From the Department of Neurology, the Section of Developmental Neurobiology,† and the Clinical Research Group for Multiple Sclerosis and Neuroimmunology,‡ University of Wuerzburg, Wuerzburg; and the Department of Neurogenetics,§ Max-Planck-Institute of Experimental Medicine, Goettingen, Germany*

It is assumed that the onset and course of autoimmune inflammatory central nervous system (CNS) disorders (eg, multiple sclerosis) are influenced by factors that afflict immune regulation as well as CNS vulnerability. We challenged this concept experimentally by investigating how genetic alterations that affect myelin (primary oligodendrocyte damage in PLPtg mice) and/or T-cell regulation (deficiency of PD-1) influence both the onset and course of an experimental autoimmune CNS inflammatory disease [MOG_{35-55}-induced experimental autoimmune encephalomyelitis (EAE)]. We observed that double pathology was associated with a significantly earlier onset of disease, a slight increase in the neurological score, an increase in the number of infiltrating cells, and enhanced axonal degeneration compared with wild-type mice and the respective, single mutant controls. Double-mutant PLPtg/PD-$1^{-/-}$ mice showed an increased production of interferon-γ by CNS immune cells at the peak of disease. Neither PD-1 deficiency nor oligodendropathy led to detectable spread of antigenic MHC class I- or class II-restricted epitopes during EAE. However, absence of PD-1 clearly increased the propensity of T lymphocytes to expand, and the number of clonal expansions reliably reflected the severity of the EAE disease course. Our data show that the interplay between immune dysregulation and myelinopathy results in a stable exacerbation of actively induced autoimmune CNS inflammation, suggesting that the combination of several pathological issues contributes significantly to disease susceptibility or relapses in human disease. ***(Am J Pathol 2009, 174:2290–2299; DOI: 10.2353/ajpath.2009.081012)***

Multiple sclerosis (MS) is a relatively frequent neurological disorder of young adults characterized by demyelination, inflammation, and axonal damage of the central nervous system (CNS).[1] Experimental autoimmune encephalomyelitis (EAE) in rodents is a widely used animal model for MS mimicking typical neurological symptoms such as paralysis and ataxia. Experimental disease as well as MS lesions are characterized by inflammation, demyelination, and accompanying axonal damage.[2] Active immunization with CNS-specific protein antigens such as myelin antigens induces $CD4^+$ Th1- and interleukin (IL)-17-dominated immune response.[3–5]

A broad variety of factors modulate the disease courses of MS and EAE. Histopathology as well as clinical course of MS shows considerable heterogeneity. Different histopathological patterns have been proposed,[6] some of which, namely pattern III and IV, include primary oligodendrocyte damage or death.[7] In the last years, several cases were described, in which mutations in the most abundant myelin protein of the CNS, proteolipidprotein (PLP), were associated with primary progressive or relapsing remitting MS.[8,9] It is therefore highly interesting to investigate how alterations in myelin proteins interplay with the immune system. Genetic variations of myelin

Supported by Sonderforschungsbereich (SFB) 581 (A3 to R.M. and A8 to H.W.), the Bildungsministerium fuer Bildung und Forschung (BMBF) (to H.W.), the Thyssen-Stiftung (10.0762.152 to R.M. and H.W.), and the Gemeinnützige Hertie Stiftung (1.01.1/07012 to R.M.).

R.M. and H.W. contributed equally to this study.

Accepted for publication February 23, 2009.

Supplemental material for this article can be found on *http://ajp.amjpathol.org*.

Present address of M.M.: Caritas Krankenhaus, Bad Mergentheim, Germany.

Address reprint requests to Prof. Heinz Wiendl, Clinical Research Group for MS and Neuroimmunology, Department of Neurology, University of Wuerzburg, Josef Schneider Strasse 11, 97080 Wuerzburg, Germany. E-mail: heinz.wiendl@klinik.uni-wuerzburg.de.

proteins might be modulators or even causative for the disease pathogenesis.

Recently, we investigated a mouse model, the transgenic PLP-overexpressing (PLPtg) mouse,[10] which spontaneously develops CNS inflammation with accumulation of both $CD11b^+$ microglial cells and $CD8^+$ T lymphocytes. The pathogenetic relevance of these cells was proven when crossbreeding PLPtg mice with RAG-1-deficient mice, which lack mature B or T lymphocytes. Absence of T lymphocytes led to an amelioration of the phenotype,[11] the pathogenetically relevant lymphocytes were clonally expanded $CD8^+$ T cells.[12]

Being aware of this context, it was interesting to investigate the influence of immune modulators in this model of primary oligodendropathy. As important candidates responsible for tissue immune homeostasis and the maintenance of tolerance we assumed members of the B7/CD28 family: T cells express co-stimulatory and co-inhibitory molecules. A co-stimulatory signal delivered by ligation of CD80 or CD86 on antigen-presenting cells (APCs) and CD28 on T cells is essential for the activation of T cells and maturation toward effector function. Other molecules are responsible for the termination of immune responses and induction or maintenance of tolerance.[13] Important members of this family of co-inhibitory molecules are programmed death (PD)-1 (CD279) and its ligands PD-L1 (B7-H1, CD274) and PD-L2 (B7-DC, CD273). PD-1 is expressed on activated T and B lymphocytes and myeloid cells. Its ligand B7-H1 is expressed on a broad variety of cells, including lymphocytes, APCs, and tissue cells such as pancreatic islet cells,[14] endothelial cells,[15] liver cells,[16] or microglial cells.[17] In contrast, PD-L2 was mainly detected on dendritic cells.[18] The PD-1/B7-H1 pathway has been studied extensively, implying a predominantly negative regulatory role. PD-1 deficient mice develop spontaneous strain-dependent autoimmune diseases such as lupus-like disease in C57/BL/6 mice[19] or autoantibody-mediated cardiomyopathy in BALB/c mice.[20] Similarly, blockade and deletion of PD-1 has been shown to result in exacerbation of diseases such as EAE,[21,22] inherited peripheral nerve,[23] and CNS demyelination,[24] diabetes,[25,26] or allograft rejection.[27]

Our group could demonstrate that a PD-1 polymorphism was associated with a progressive disease course of MS,[28] indicating that PD-1 acts as a disease-modifying factor in human autoimmunity. Genetic ablation of B7-H1 (PD-L1) is associated with an accelerated and worsened EAE disease course,[29] a consequence of the limited ability of CNS parenchymal cells to restrict CNS-specific immune responses via the B7-H1/PD-1 pathway.[29,30] Thus, a functional PD-1/B7-H1 pathway is an important regulator of immune homeostasis and tissue tolerance.

In the present study, we investigated how the combination of genetic alterations affecting myelin (primary oligodendrocyte damage in PLPtg mice) and/or affecting T-cell regulation (PD-1 deficiency) influence the onset and course of an experimental autoimmune CNS inflammatory disease [myelin oligodendrocyte glycoprotein $(MOG)_{35-55}$ induced EAE]. This experimental setup could mimic a situation in which genetics predispose a combination of a CNS vulnerability factor (myelinopathy) together with an immune regulatory impairment (PD-1 dysfunction) and encounter an acute CNS-directed inflammatory response. We demonstrate that combined pathology leads to a very stable and accelerated experimental autoimmune CNS inflammation.

Materials and Methods

Animals and Determination of Genotypes

PLP transgenic mice[10] were bred and genotyped as described previously.[11] In short, the transgene was polymerase chain reaction (PCR)-amplified using the primer set 5′-CAGGTGTTGAGTCTGATCTACACAAG-3′ and 5′-GCATAATACGACTCACTATAGGGGATC-3′ with an annealing temperature of 55°C and an elongation time of 45 seconds at 72°C. PD-$1^{-/-}$ mice[31] were genotyped as previously described with the primer pair 5′-CCGCCTTCTGTAATGGTTTG-3′ and 5′-TGTTGAGCAGAAGACAGCTAGG-3′ for the wild-type allele, an annealing temperature of 54°C, and an elongation time of 45 seconds. The knockout allele was detected with the primer pair 5′-GCCCGGTTCTTTTTGTCAAGACCGA-3′ and 5′-ATCCTCGCCGTCGGGCATGCG CGCC-3′ at an annealing temperature of 60°C and an elongation time of 45 seconds. PCR products were visualized on an agarose gel with the wild-type band at 690 bp and the knockout band at 400 bp. PLPtg mice were crossbred with PD-$1^{-/-}$ mice. All mice were bred on a C57/BL/6 background for more than 10 generations and all animal experiments were approved by the local authorities (Regierung von Unterfranken, experiment number 54-2531.01-36/06).

Induction and Scoring of EAE

Active EAE was induced in age- and sex-matched littermate mice by subcutaneously injecting 100 μg of MOG_{35-55} peptide (EVGWYRSPFSRVVHLYRNGK; synthesized and high performance liquid chromatography-purified by Rudolf Volkmer, Charite, Berlin, Germany) as described previously.[29] MOG_{35-55} peptide was emulsified with an equal volume of complete Freud's adjuvant, containing *Mycobacterium tuberculosis* H37RA (Difco, Detroit MI) at a final concentration of 1 mg/ml. Additionally, the mice received two intraperitoneal injections of pertussis toxin (400 ng per mouse; List Biological Laboratories, Campbell, CA) at the time of immunization and 48 hours later. Mice were weighed and observed daily for clinical signs and scored based on the following scale (EAE score): 0, no disease; 1, limp tail; 2, hind limp weakness; 3, hind limp paralysis; 4, hind and fore limp paralysis; 5, moribund or death. Scores are shown as mean daily clinical scores for all mice per group (n = 4 to 6 per group).

Purification of Splenocytes

Splenocytes were harvested as described before[11,12] by passing them through a 70-μm cell strainer (BD Bio-

sciences Pharmingen, San Jose, CA). Erythrocyte lysis was performed with a hypo-osmolar lysis buffer (150 mmol/L NH_4Cl_2, 10 mmol/L $KHCO_3$, 0.1 mmol/L ethylenediaminetetraacetic acid in distilled water at pH 7.3) for 5 minutes at room temperature. Afterward, cells were washed and processed for consecutive experiments.

Purification of Mononuclear Cells from Cervical Lymph Nodes

Cervical lymph nodes were prepared and the tissue was disrupted by grinding between object trays. Cells were then passed through a 40-μm cell strainer (BD Biosciences Pharmingen). Afterward, cells were washed and processed for the respective experiments.

Preparation of CNS Mononuclear Cells

Mice were euthanized with CO_2 and transcardially perfused with cold 0.1 mol/L phosphate-buffered saline (PBS). The brains were dissected and the spinal cords were flushed out with PBS by hydrostatic pressure. Afterwards, CNS tissue was homogenized, washed, and separated over a cold Percoll (Amersham Biosciences, Freiburg, Germany) gradient. Cells were harvested from the 30 to 50% Percoll interface, washed, and used for following experiments.

Tissue Preparation and Immunohistochemistry

For identification of $CD11b^+$ macrophage-like cells, mice were transcardially perfused with 4% paraformaldehyde in 0.1 mol/L cacodylate followed by tissue dissection of optic nerves and spinal cords from the brainstem to the lumbar regions, postfixation in the same fixative for 2 hours, and cryoprotection in 30% sucrose overnight. Alternatively, mice were perfused with 0.1 mol/L PBS followed either by direct snap-freezing of the dissected tissue (for $CD4^+$ and $CD8^+$ T-lymphocyte immunohistochemistry) or postfixation in 4% paraformaldehyde in PBS for 2 hours (for neurofilament immunohistochemistry) and then subsequent embedding in Tissue-Tek OCT compound (Miles Laboratories, Elkhart, IN). After snap-freezing, 10-μm-thick longitudinal sections of the optic nerves and transverse sections of the spinal cords were cut. For immune cell analysis, lumbar spinal cords were used, whereas for neurofilament immunohistochemistry, sections were taken from the beginning of the cervical enlargement to ensure that the same regions were analyzed in all mice.

Immunohistochemical stainings were performed as described before.[11,32] Nonspecific binding was blocked for 30 minutes in 5% normal bovine serum and then sections were incubated with the primary antibodies diluted in 1% normal bovine serum (overnight, 4°C). Activated macrophage-like cells were detected with rat anti-mouse CD11b (Serotec, Oxford, UK); rat anti-mouse CD4 (Serotec) and rat anti-mouse CD8 (Chemicon, Temecula, CA) antibodies were used for the identification of T lymphocytes. To identify all axons (myelinated and demyelinated), sections were incubated with antibodies against phosphorylated neurofilament (SMI-31; Sternberger Monoclonals, Lutherville, MD) and nonphosphorylated neurofilament (SMI-32) in combination or alone. Detection of primary antibodies was achieved by using a biotinylated secondary antibody to rat Igs (macrophage-like cells, T-cell antibodies) or mouse Igs (SMI-31 and SMI-32) for 1 hour, followed by avidin/biotin reagent (DAKO, Carpinteria, CA) before incubation and staining with diaminobenzidine-HCl (DAB) and H_2O_2. The specificity was controlled by omission of the primary antibodies.

Quantification of Immune Cells and Axons in the CNS

Lumbar spinal cord cross sections and longitudinal sections of the optic nerve of wild-type, PD-$1^{-/-}$, PLPtg, and PLPtg/PD-$1^{-/-}$ mice were examined. Quantification of $CD4^+$, $CD8^+$, and $CD11b^+$ cells was performed in longitudinal sections of the complete optic nerve or lumbar sections of the spinal cord using a Zeiss (Oberkochen, Germany) Axiophot2 microscope at a final magnification of $\times$300. The number of positively labeled cells was calculated per mm^2. The area was measured using digital images acquired via a charge-coupled device camera and ImagePro 4.0 software (Media Cybermetics, Silver Spring, MD). Axonal density was determined within preselected fields (500 μm^2 in area) at specific sites within the dorsal column (cuneate fasciculus), dorsal corticospinal tract, as well as in ventral and lateral fasciculus. Stained axons were counted using MetaVue Software (Molecular Devices, Downingtown, PA).

Enzyme-Linked Immunosorbent Assay (ELISA)

Splenocytes (1×10^6) were cultured overnight with and without MOG_{35-55} peptide (10 μg/ml). After 24 hours, the supernatant was collected and analyzed by ELISA (R&D Systems, Minneapolis, MN) according to the manufacturer's recommendations. Readout was performed with an Original Multiskan EX ELISA reader (Labsystems, Helsinki, Finland).

ELISPOT Assays

Splenocytes, lymph nodes, and CNS-derived lymphocytes were investigated during the priming phase (day 7 after immunization), the peak of disease (approximately day 15), and in the late phase of disease (day 20). CNS lymphocytes (5×10^4) or 1×10^5 lymph node lymphocytes or splenocytes per well were incubated for 24 hours in provided 96-well plates, unstimulated or stimulated with either MOG_{35-55} peptide (10 μg/ml), mixed MHC class I restricted peptides (PLP peptides: VCGSNLLSI, AATYNFAVL, ATYNFAVL, NYQDYEYL; MOG peptides: LIICYNWL, VGLVFLFL, SPGKNATGM, FYWVNPGVL; one MBP peptide: ADPGNRPHL; from Genscript Corp., Piscataway, NJ, used at 200 nmol/L or five mixed MHC class

II restricted peptides: $MOG_{113-127}$ (LKVEDPFYWVSPGVL), $MOG_{120-134}$ (YWVSPGVLTLIALVP), $MOG_{183-197}$ (FVIVPVLGPLVALII), MBP_{54-72} (SHHAARTTHYGSLPQKSQR), $PLP_{178-191}$ (NTWTTCQSIAFPSK) (from EMC Microcollections, Tuebingen, Germany). Interferon (IFN)-γ and IL-17 ELISPOT assays were performed according to the manufacturer's instructions (BD Pharmingen, San Diego, CA; R&D Systems). Spots were quantified by CTL Europe (Aalen, Germany) using ImmunoSpot 4.0.17.

Spectratyping

The CDR3 spectratyping with the corresponding primers was performed as described previously.[12,33] Briefly, PCR with a Cβ-specific reverse primer and 24 Vβ-specific forward primer was performed on cDNA transcribed from 500 ng of leukocyte mRNA derived from spleens or CNS. The following PCR steps were applied: 94°C, 1 minute; 94°C, 1 minute 10 seconds; 60°C, 1 minute; 72°C, 4 minutes (40 steps); 72°C, 10 minutes. Thirteen fluorescence-labeled reverse primers (12 Jβ, 1 Cβ) were used to label each Vβ-Cβ PCR product during PCRs. The PCR steps were: 94°C, 2 minutes, 60°C, 1 minute, 72°C, 15 minutes (five steps). The labeled PCR products (Vβ-Jβ, Vβ-Cβ) were analyzed on an ABI Prism 3130 capillary sequencer (Applied Biosystems, Foster City, CA) regarding their length and distribution, using a module for fragment analysis. As an internal length standard, 500-ROX (Applied Biosystems) was applied for every sample.

Statistical Analysis

The unpaired two-tailed Student's *t*-test was used for comparison of quantified profiles. Scores were analyzed by using the nonparametric Mann-Whitney *U*-test and the Kruskal-Wallis test.

Results

Absence of PD-1 Alters Onset of EAE

To investigate the influence of combined primary oligodendrocyte damage and a defective T-cell inhibition on the EAE disease course, we immunized PLPtg/PD-1$^{-/-}$ mice with MOG_{35-55} peptide. As controls we used wild-type, PD-1$^{-/-}$, and PLPtg mice. After titration experiments with different doses of antigen (data not shown), experiments were performed with a relatively low dose of MOG_{35-55} peptide (100 μg) to detect putatively higher susceptibilities for the disease, especially because PD-1 is known to act mainly under submaximal stimulatory conditions.

Mice with a combined pathology (PLPtg/PD-1$^{-/-}$ mice) had an earlier onset of disease, as reflected by the disease course, the relative number of normal appearing mice after immunization, and the mean day of onset (Table 1), which was significant in all experiments compared with wild-type mice. In addition, assessment of the EAE score always revealed a significantly more pronounced disease onset in PLPtg/PD-1$^{-/-}$ double mutants compared with the wild-type control group (Table 1; Figure 1, A and B).

Table 1. Significantly Earlier Onset of Disease in PLPtg/PD-1$^{-/-}$ Mice

Group	Mean day of onset*	Mean maximal score†	Median‡
wt	13.3 ± 2.2	2.9 ± 0.3	3.0
PD-1$^{-/-}$	12.4 ± 1.7	3.6 ± 1.1	4.0
PLPtg	11.8 ± 2.6	2.0 ± 1.2	2.5
PLPtg/PD-1$^{-/-}$	10.6 ± 0.8§**	2.6 ± 0.0	2.5
wt	17.0 ± 3.3	2.8 ± 0.5	2.0
PD-1$^{-/-}$	12.5 ± 2.6§**	3.3 ± 0.9	3.0
PLPtg	14.0 ± 3.1	2.6 ± 0.4	2.5
PLPtg/PD-1$^{-/-}$	10.5 ± 2.3§††	2.8 ± 0.3	3.0
wt	13.3 ± 2.3	2.1 ± 1.2	2.5
PD-1$^{-/-}$	11.5 ± 1.1	1.9 ± 1.1	2.5
PLPtg	13.3 ± 2.3	1.7 ± 1.1	2.5
PLPtg/PD-1$^{-/-}$	10.9 ± 1.8§‖**	2.8 ± 0.4¶‖**	3.0
wt	12.5 ± 0.6	1.1 ± 1.0	1.0
PD-1$^{-/-}$	10.6 ± 1.8	2.9 ± 0.4§**	3.0
PLPtg	11.2 ± 1.3	3.0 ± 0.5§**	3.0
PLPtg/PD-1$^{-/-}$	10.6 ± 0.9§††	3.4 ± 0.2§‡‡,‖**	3.5
wt	12.8 ± 1.6	0.8 ± 0.6	1.0
PD-1$^{-/-}$	11.3 ± 2.2	2.2 ± 0.8§‡‡	2.5
PLPtg	11.2 ± 2.4	1.7 ± 0.6§‡‡	1.5
PLPtg/PD-1$^{-/-}$	10.6 ± 2.1§††	2.3 ± 0.8§‡‡	2.5
wt	13.3 ± 1.5	1.8 ± 1.4	1.8
PD-1$^{-/-}$	12.8 ± 2.1	2.0 ± 1.1	2.0
PLPtg	13.0 ± 1.0	1.0 ± 0.6	1.0
PLPtg/PD-1$^{-/-}$	11.6 ± 0.6§,‖**	2.7 ± 0.6‖††	2.5
wt	12.4 ± 1.5	1.7 ± 1.4	2.0
PD-1$^{-/-}$	12.4 ± 1.4	2.6 ± 1.2	3.3
PLPtg	11.3 ± 1.7	1.9 ± 0.9	2.3
PLPtg/PD-1$^{-/-}$	9.5 ± 1.2§,‖‡‡¶††	3.4 ± 0.8§‖††	3.5

*Mean day of disease onset was calculated only for the mice that developed EAE during the time of investigation. Note significantly earlier onset of disease in PLPtg/PD-1$^{-/-}$ mice compared with wild-type (wt) mice. Mean maximal score (†) and median (‡) were calculated for all mice in the group.

§Significant differences compared with wild-type mice (Student's *t*-test).

¶Significant differences compared with PD-1$^{-/-}$ mice.

‖Significant differences compared with PLPtg mice. Data represent mean ± SD, n = 3 to 8 per group.

P values ≤0.05 were considered significant,** P value <0.05, †† P value ≤0.01, ‡‡ P value ≤0.001.

PD-1$^{-/-}$ mice usually showed a similar disease course like PLPtg/PD-1$^{-/-}$ mice, but displayed much broader interindividual variations with a slightly delayed disease onset compared with double mutants. Initially, the slope of the disease curve developed similarly in wild-type and PLPtg mice. After ~15 to 20 days, all groups exhibited comparable disease scores (Table 1, Figure 1A) with slightly higher levels in the absence of PD-1. Nevertheless, when comparing the mean maximal score, in five of seven experiments, PLPtg/PD-1$^{-/-}$ mice showed a significantly higher mean maximal score. Disease incidence and mortality rate, which was generally low, did not differ significantly between the groups. Taken together, PLPtg/PD-1$^{-/-}$ mice developed disease significantly earlier and reached a higher mean maximal score compared with wild-type mice.

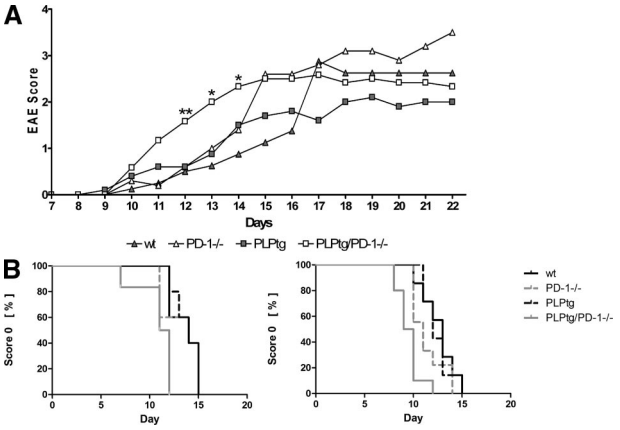

Figure 1. PLPtg/PD-1$^{-/-}$ mice show earlier and more pronounced onset of EAE. **A:** Wild-type (wt), PD-1$^{-/-}$, PLPtg, and PLPtg/PD-1$^{-/-}$ mice were immunized with MOG_{35-55}. PLPtg/PD-1$^{-/-}$ show a significantly earlier onset and stronger disease course compared with wild-type mice. At later time points, EAE disease scores are similar in all groups, as reflected by lack of statistical significance. The figure shows one representative of seven experiments. $^{*}P < 0.05$, $^{**}P = 0.01$. $n = 5$ mice per group. **B:** Relative number of mice displaying no clinical alterations (score 0) after immunization. These two representative experiments clearly reflect early onset of disease in PLPtg/PD-1$^{-/-}$ mice ($n = 5$ mice per group).

Absence of PD-1 and Overexpression of PLP Is Associated with Increased Numbers of Immune Cells in the CNS

To quantify lymphocytes and macrophage-like cells in neural tissue, immunohistochemistry for CD4, CD8, and CD11b was performed on cross sections of the lumbar spinal cord and longitudinal sections of the optic nerve during EAE. CD4^{+} cells were significantly more frequent in spinal cords of PLPtg/PD-1$^{-/-}$ mice compared with wild-type mice. PLPtg and PD-1$^{-/-}$ mice both showed higher amounts than wild-type mice, but differences were not statistically significant (Figure 2A). A similar trend lacking statistical significance was detectable in optic nerves (Figure 2B). In contrast, CD8^{+} lymphocytes were significantly elevated both in spinal cord (Figure 2C) and optic nerve (Figure 2D) in PLPtg/PD-1$^{-/-}$ mice compared with wild-type mice. Regarding the spinal cord, PLPtg and PD-1$^{-/-}$ single mutants showed a stronger accumulation of cells than wild types. CD11b^{+} macrophages were also significantly more frequent in spinal cords of PLPtg/PD-1$^{-/-}$ mice compared with wild-type mice (Figure 2, E and F), which was neither detectable in PLPtg and PD-1$^{-/-}$ mice nor in optic nerves of all groups (Figure 2G). Healthy mice which were investigated at the same age (2 months) did not show significant differences between the genotypes for CD4^{+} (Figure 2H) and CD8^{+} (Figure 2I) lymphocytes and CD11b^{+} macrophage-like cells (Figure 2J). Taken together, combined pathology is associated with higher numbers of CD4^{+} and CD8^{+} T cells and higher numbers of macrophages in the spinal cord of EAE mice.

Double-Mutant PLPtg/PD-1$^{-/-}$ Mice Exhibit Highest Axonal Loss during EAE

To determine whether differences in the CNS-infiltrating T cells and macrophages in double mutants were associated with more pronounced axonal damage we performed quantitative immunohistochemistry against phosphorylated and nonphosphorylated neurofilament in the cervical spinal cord 50 days after induction of EAE. A significant reduction of total neurofilament was observed in the absence of PD-1 (independent from the absence or presence of the PLP transgene) in the ventral, lateral, and dorsal funiculus and in the corticospinal tract. Interestingly, the amount of defective, nonphosphorylated neurofilament was highest in PLPtg/PD-1$^{-/-}$ mice, which was significant compared with wild-type mice in all investigated areas and for the dorsal funiculus and in the corticospinal tract compared with PD-1$^{-/-}$ and PLPtg mice, thereby reliably reflecting the clinical score in these mice (Figure 3, A and B).

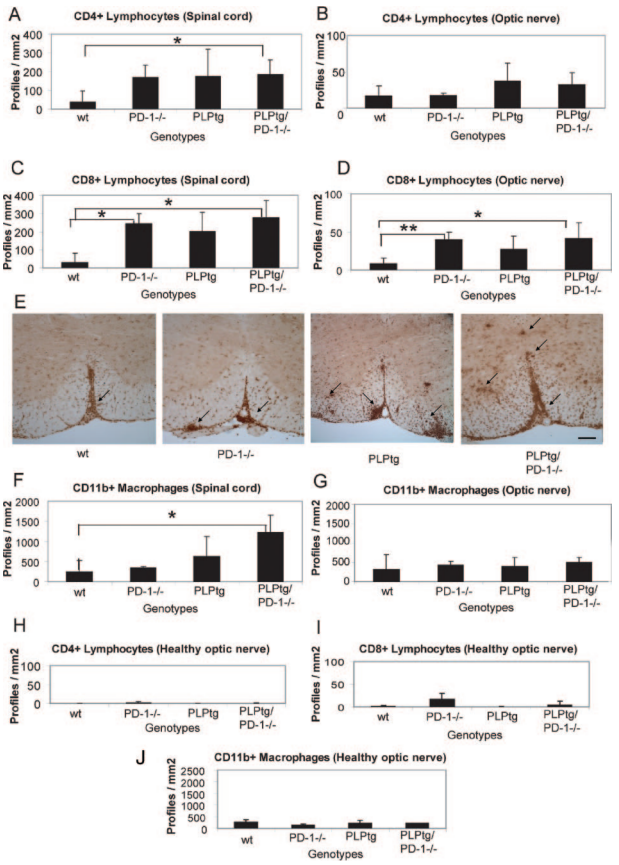

Figure 2. PLPtg/PD-1$^{-/-}$ mice show elevated numbers of immune cells in the CNS. Quantification of immune cells in the spinal cord (**A**, **C**, **F**) and optic nerve (**B**, **D**, **G**) of wild-type (wt), PD-1$^{-/-}$, PLPtg, and PLPtg/PD-1$^{-/-}$ mice at the peak of disease ($n = 3$ to 5). Quantification includes CD4^{+} (**A**, **B**) and CD8^{+} (**C**, **D**) lymphocytes and CD11b^{+} macrophages (**F, G**). **E:** Representative CD11b immunohistochemistry on cross-sections of the ventral part of lumbar spinal cord. **Arrows** indicate accumulation of CD11b^{+} macrophages. **H–J:** Quantification of CD4^{+} (**H**) and CD8^{+} (**I**) lymphocytes and CD11b^{+} macrophage-like cells (**J**) in healthy mice of the same age. Error bars represent standard deviations. $^{*}P < 0.05$, $^{**}P \leq 0.01$. Scale bar = 200 μm.

Absence of PD-1 Is Associated with Higher Production of IFN-γ by Splenocytes during the Early Phase of Disease

We next investigated whether differences in the production of proinflammatory cytokines were associated or re-

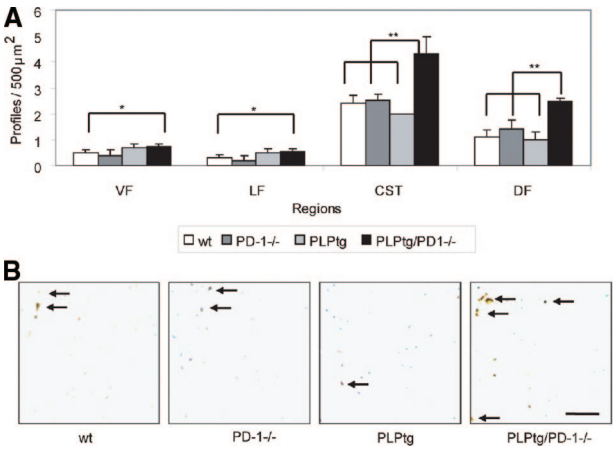

Figure 3. PLPtg/PD-1$^{-/-}$ mice show elevated numbers of dephosphorylated neurofilament in the spinal cord. **A:** Quantification of nonphosphorylated neurofilament in the cervical spinal cord of wild-type (wt), PD-1, PLPtg, and PLPtg/PD-1$^{-/-}$ mice (n = 3 to 4). Investigated areas include ventral funiculus (VF), lateral funiculus (LF), corticospinal tract (CST), and dorsal funiculus (DF). **B:** Representative examples of SMI32^{+} swollen axonal profiles in the spinal cord (**arrows**). Error bars represent standard deviations. $^{*}P < 0.05$, $^{**}P \leq 0.01$. Scale bar = 10 μm.

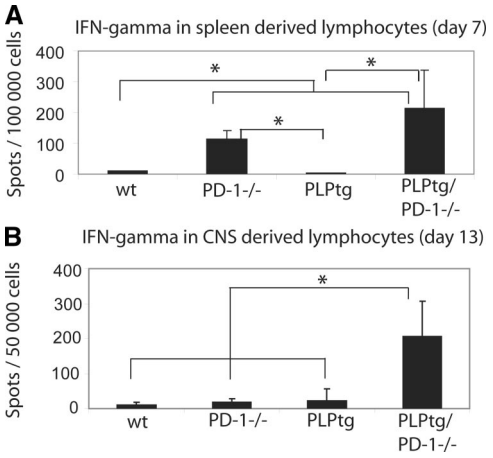

Figure 4. CNS-derived cells from PLPtg/PD-1$^{-/-}$ mice produce higher amounts of IFN-γ^{+} at the peak of disease. IFN-γ ELISPOT assays were performed on splenocytes (**A**) and CNS-derived lymphocytes (**B**) under restimulation with MOG_{35-55}. **A:** Higher amounts of IFN-γ^{+} cells were detected in PD-1$^{-/-}$ and PLPtg/PD-1$^{-/-}$ mice in the early phase of EAE (day 7). **B:** IFN-γ^{+} cells are significantly more frequent in PLPtg/PD-1$^{-/-}$ at the peak of disease (day 13). In these experiments, lymphocytes were pooled from three mice per group. $^{*}P < 0.05$.

sponsible for the observed differences. IFN-γ was measured as an indicator cytokine strongly regulated during EAE and closely correlated to CNS damage.[34] To first elucidate if PD-1 influences the secretion of IFN-γ during EAE, we investigated the IFN-γ levels by ELISA in the supernatant of splenocytes from wild-type and PD-1$^{-/-}$ mice at different time points of disease. At day 7 after immunization, before the actual onset of disease, significantly more IFN-γ was secreted by PD-1$^{-/-}$ splenocytes after re-stimulation with MOG_{35-55} peptide (see Supplemental Figure S1A at *http://ajp.amjpathol.org*).

At the peak of disease (day 13), there was still a trend toward a higher production of IFN-γ by PD-1$^{-/-}$ splenocytes and the amounts of secreted IFN-γ had substantially increased, but this was no longer significant (see Supplemental Figure S1B, see *http://ajp.amjpathol.org*). In the late phase of the disease (day 17), PD-1$^{-/-}$ splenocytes did not produce detectable levels of IFN-γ and also the amount in wild-type splenocytes dropped to levels comparable with day 7 (see Supplemental Figure S1C, see *http://ajp.amjpathol.org*).

Double-Mutant PLPtg/PD-1$^{-/-}$ Mice Show Increased Production of IFN-γ in the CNS at the Peak of Disease

To investigate the production of IFN-γ in detail, we harvested lymphocytes from the CNS, cervical lymph nodes, and the spleen at various time points after immunization in the different genotypes. Moreover, we used a highly sensitive Elispot assay. In the early phase of disease (day 7), when stimulated with MOG_{35-55}, IFN-γ production was significantly elevated in splenocytes of PD-1$^{-/-}$ and PLPtg/PD-1$^{-/-}$ mice compared with wild-type and PLPtg mice (Figure 4A). At later phases of disease (day 15 after immunization), splenocytes of all groups exhibited a strong IFN-γ response when stimulated with MOG_{35-55}, which did not differ significantly between the groups (data not shown).

A delayed pattern of IFN-γ production could be observed in lymphocytes derived from cervical lymph nodes restimulated with MOG_{35-55}. At day 7, only low amounts of cells produced IFN-γ and the amount of cells did not differ between the genotypes. After the onset of disease (day 10 after immunization) the IFN-γ production was primarily increased. At that time point, PLPtg/PD-1$^{-/-}$ mice show significantly more IFN-γ^{+} cells than wild-type mice. Later, at day 15 after immunization, PLPtg/PD-1$^{-/-}$ mice still produced significantly more IFN-γ than wild-type and PLPtg mice but the total number of positive cells was reduced to very low levels (data not shown).

Interestingly, at the peak of disease (day 13), the amount of IFN-γ^{+} cells on MOG_{35-55} stimulation in CNS-derived lymphocytes was significantly higher in cells from PLPtg/PD-1$^{-/-}$ mice than in all other groups (Figure 4B), which might reflect the highest maximal score in these mutants. In the later phase of the disease, the IFN-γ production in the CNS was reduced in double mutants while it increased in the other genotypes, leading to a significantly higher amount in wild-type and PD-1$^{-/-}$ cells compared with PLPtg/PD-1$^{-/-}$ (data not shown).

These data indicate that absence of PD-1 is associated with higher peripheral MOG-specific IFN-γ secretion. This systemic difference is only observable in the preclinical phase of EAE. However, combined pathology is associated with a significantly higher secretion of IFN-γ by CNS-MOG-specific T cells at peak of disease.

Absence of PD-1 or Oligodendropathy Does Not Lead to Detectable Spread of Antigenic MHC Class I or Class II Restricted Epitopes during EAE

We reasoned whether EAE in PLPtg mice or in PD-1$^{-/-}$ mice would be associated with early epitope spreading

against various CNS antigens, either restricted by MHC class I or MHC class II molecules. This has been elegantly shown in several models of EAE, especially in SJL mice immunized with PLP peptides.[35] We therefore tested animals at the peak of disease for reactivity against a number of MHC class II-related myelin peptides ($MOG_{113-127}$, $MOG_{120-134}$, $MOG_{183-197}$, MBP_{54-72}, $PLP_{178-191}$).[36] However, no relevant MHC class II restricted responses against other myelin peptides than MOG_{35-55} were detectable (data not shown). Because the pathogenic inflammatory response in PLPtg mice is mediated by $CD8^+$ T cells[11,12] we also tested for responses after antigenic stimulation with a number of MHC class I myelin peptides mentioned in the *Materials and Methods*.[12] However, no responses were measured (data not shown).

Absence of PD-1 Increases Clonal Expansions of T Cells during EAE

To assess the T-cell receptor repertoire during MOG EAE in BL/6 wild-type, PD-$1^{-/-}$, PLPtg, and PLPtg/PD-$1^{-/-}$ mice, we used CDR3 spectratyping analysis on CNS- and spleen-derived lymphocytes.[12] This PCR-based method allows detection of mono- and oligoclonal expansions of T cells in different tissues.

CNS-derived lymphocytes were assessed for clonal expansions and distributions ($n = 3$ mice per group). In wild-type mice peak numbers of 8 ± 1.7 were detected. This was similar to the number found in EAE of PLPtg mice (9.3 ± 4.7). Absence of PD-1 clearly increased the propensity of T lymphocytes to expand: In PD-$1^{-/-}$ mice, 17 ± 7.8 peaks were detected compared with 15.3 ± 2.5 in PLPtg/PD-$1^{-/-}$ double mutants. When applying statistical analysis to peak numbers, a significant difference was only detectable between wild-type and PLPtg/PD-$1^{-/-}$ mice ($P = 0.01$), which was attributable to high variations in PD-$1^{-/-}$ mice and again a sign of very homogeneous disease in the double mutants. Additionally, the number of clonal expansions reliably reflected the severity of the EAE disease course.

In other mouse strains (eg, B10.PL), it has been shown that so called public clones, which are T cells with the same Vβ, Jβ, CDR3 length and the same or similar CDR3 amino acid sequence, which are present in each animal, are responsible for driving EAE.[37] Our analysis firstly describing CDR3 spectratyping in MOG_{35-55}-induced EAE in C57/B6 mice revealed a higher variability of clonal expansions in different mice.

Here, the expansions clustered in several Vβ regions: Vβ 1: 23%; Vβ 5.2: 8%; Vβ 10: 16%; Vβ 11: 22%; Vβ 16: 9%; of all observed expansions, meaning that 5 Vβ regions (of 24) included 78% of all expansions (Figure 5). However, no defined Vβ/Jβ expansion was present in all analyzed animals. In examples of Vβ/Jβ combinations, which could be found in several animals (eg, Vβ1/Jβ2.5, found in 7 of 12 animals), the CDR3 length varied slightly and proved the difference on the clonal level. Interestingly, we found the Vβ/Jβ combination (Vβ11/Jβ1.1) of the MOG-specific 2D2 T cells[38] in the CNS of 5 of 12 animals. However, the CDR3 length of these clones was not identical, suggesting differences in the antigen specificity. When compared with the spleen TCR repertoire, it became evident that the vast majority of peaks were CNS-restricted. The corresponding spleen spectratypes also always showed peaks, but the peak number was ~20% of that in the CNS (data not shown).

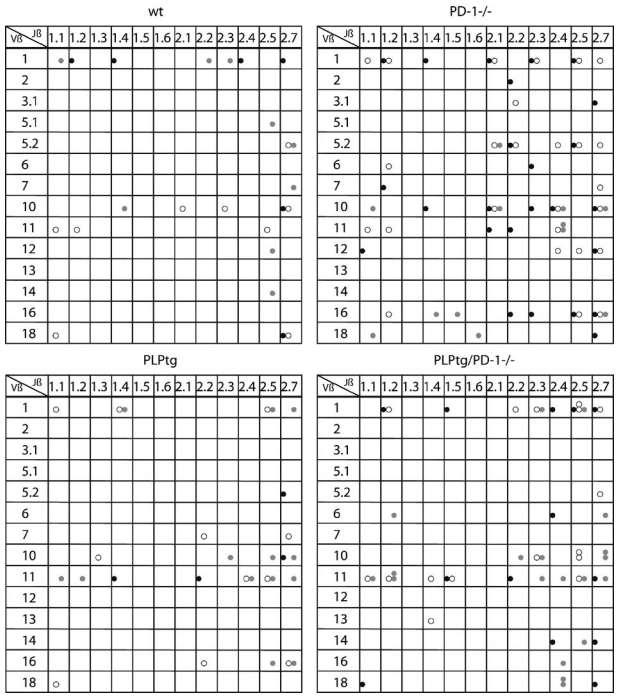

Figure 5. Spectratyping analysis of T-cell receptors in CNS-derived lymphocytes. The T-cell receptor repertoire of lymphocytes from the CNS of wild-type, PD-$1^{-/-}$, PLPtg, and PLPtg/PD-$1^{-/-}$ ($n = 3$) mice in the late phase of EAE (day 18) was analyzed by spectratyping. Clonal expansions (visible as single peaks in the fragment analysis) are shown as dots (different gray scales indicate individual animals). The expanded T cells are characterized by their Vβ- and Jβ-chains (Vβ, rows; Jβ, columns). The clonal expansions occurred widely distributed over different Vβ and Jβ regions, although some domains seemed to be prone for clonal expansions in different mutant mice.

Discussion

We here investigated how genetic predisposition for myelin damage (PLPtg overexpression) combined with aberrant T cell regulation (PD-1 deficiency) influence the onset and course of an experimental autoimmune CNS disease (MOG_{35-55}-induced EAE). We observed that double pathology was associated with a significantly earlier onset of EAE, a slight increase in the neurological score, an increase of infiltrating cells, and enhanced neuronal degeneration compared with wild-type mice. Thus PLP overexpression and PD-1 deficiency have a confounding effect on CNS inflammation. The double mutants also displayed an earlier onset in comparison with PD-$1^{-/-}$ and PLPtg single mutants (Figure 1B), but because of high individual variability of the single mutants, the corresponding differences failed to reach statistical significance.

The less homogenous disease onset and course in PD-$1^{-/-}$ single mutants and the lack of statistically significant differences compared with wild-type mice might

be caused by the low dose of antigen we used to induce the disease. Under these conditions, only the presence of two predisposition factors led to homogenous disease course. Most likely, at least two different disease mechanisms were acting in the immunized double mutants. First, the underlying primary oligodendrocyte damage might have induced an enhanced vulnerability and, possibly, tissue instability. Second, the absence of the coinhibitory molecule PD-1 induced a stronger inflammatory stimulus, and the combination of both culprits resulted in the accelerated, stable, homogenous exacerbation of disease. Importantly, the combination of the two factors without EAE induction already led to an aggravation of myelin and axon damage[24] but at a much later time point. It is tempting to speculate that, in the young double mutants, a not yet visible predisposition for severe inflammatory disease progression already exists and becomes triggered by EAE induction. It is of note that the earlier and stronger onset of disease is followed by a parallel disease course of all groups and absence of significant differences. Nevertheless, the mean maximal score was significantly higher in PLPtg/PD-1$^{-/-}$ double mutants compared with wild-type mice in the vast majority of experiments.

The significance of combined pathology is reflected not only by the disease course, which is most prominent in the double mutants, but also by the accumulation of CD4$^+$ and CD8$^+$ lymphocytes and CD11b$^+$ macrophages in the CNS. Here, the highest amount is always detected in double mutants, whereas the presence of one single pathological feature (PLPtg or PD-1$^{-/-}$) is sufficient to induce increased cell numbers compared with the wild-type level.

In this context, it is interesting that the demyelination in PLPtg mice is clearly mediated by CD8$^+$ lymphocytes,[11] whereas EAE is mainly depending on CD4$^+$ lymphocytes. It is therefore plausible to assume that the increased cell numbers in PLPtg compared with wild-type mice are mainly triggered by the underlying oligodendrocyte damage. Recent studies have shown a predominance of CD8$^+$ T lymphocytes in MS lesions.[39] The fact that EAE is predominantly mediated by CD4$^+$ T lymphocytes supports the view that a direct comparison with MS is a limited possibility.[40] It would, therefore, be challenging to perform similar experiments by using a CD8$^+$ T lymphocyte-mediated MS model.

It was another important finding that the immune response in the investigated mice was always directed primarily against MOG$_{35-55}$, which had been used for immunization, and we could not detect any reactivity toward other myelin peptides. This does not entirely exclude the presence of epitope spreading, but at least none of the predicted MHC class I or II peptides we investigated was recognized by CNS-infiltrating T cells within the experimental window.

Another important feature, which faithfully reflected the clinical phenotype of the mice, was the amount of nonphosphorylated neurofilament (reflecting axon injury[41]), which was highest in PLPtg/PD-1$^{-/-}$ mice and resembles enhanced neuronal damage in the presence of mice with double pathology. The stronger susceptibility of PD-1 deficient immune cells to proliferate and produce cytokines was reflected not only by the higher amount of IFN-γ production by PD-1 deficient compared with wild-type splenocytes but also by the increased number of IFN-γ producing CNS cells in ELISPOT assays in PLPtg/PD-1$^{-/-}$ mice. Disruption of the PD-1/PD-L1 pathway may therefore be a critical event for the production of IFN-γ within the CNS, as it is for the disease score in EAE.[21,22,29]

The strong influence of PD-1 on T-cell homeostasis is also reflected by the number of peaks in our clonality analysis (spectratyping analysis). Oligoclonal expansions, which can account for strong immune activation against a specific antigen, were present in all investigated mice and genotypes. We have shown in previous experiments that healthy 12-month-old wild-type mice do not display any clonal expansions neither in spleen nor in CNS-derived lymphocytes whereas PLPtg mice always showed one Vβ expansion, which differed in size and location.[12]

When investigating healthy 12-month-old PD-1$^{-/-}$ and PLPtg/PD-1$^{-/-}$ mice, we always detected higher numbers of peaks,[6–9] indicating oligoclonal expansions, but no significant differences between these two groups.[24] To our knowledge, this is the first study describing clonal expansions in BL/6 mice during EAE. Interestingly, there was no difference in the number of oligoclonal expansions between PLPtg and wild-type mice, which both displayed approximately eight to nine oligoclonal expansions, whereas in the absence of PD-1, independent from an additional myelin mutation, the number was approximately twice as high (17 and 15, respectively). In line with our results describing the homogeneous disease course in PLPtg/PD-1$^{-/-}$ mice, these mice displayed only a very limited variability of different Vβ/Jβ types in the spectratyping analysis. Therefore one might speculate that the immunological and pathological response gets focused or stabilized in the presence of a factor predisposing for CNS vulnerability (PLPtg) in addition to factors impairing T-cell homeostasis (lack of PD-1). We suggest that transgenic overexpression of myelin molecules in PLP transgenic mice thus amplified and focused the CNS-directed immune response observed after immunization with MOG. This assumption is supported by the highly altered clonal expansion patterns observed in mice bearing a double pathology in comparison with PD-1 deficient mice alone. Of note, neither deficiency of PD-1, nor the combination with PLPtg influenced epitope restriction or promoted epitope spreading under the given experimental conditions.

This indicates that under the dominant immune stimulus of EAE induction, subtle differences (myelin) are no longer visible while a general immune dysregulation can enhance the severity of disease and immune reaction. Nevertheless, it is interesting that—as opposed to B10.PL mice[37]—the reaction toward a common antigen in BL/6 mice results in diverse and not identical clonal expansions.

Taken together, investigating the course and the immunopathogenetic features of MOG$_{35-55}$-induced EAE in a model combining both oligodendrocyte-related myeli-

nopathy and PD-1 dependent alteration of immune responses can provide interesting insights in the modulation of autoimmune diseases. Our data suggest that the interplay between immune dysregulation and myelinopathy results in a stable exacerbation of the disease. The PD-1$^{-/-}$ mutation alone led to a stronger exacerbation of EAE than in wild-type mice, but was characterized by a striking clinical and pathological variability within the group. This variability was not seen in mice bearing double pathology. Our observation might be of clinical relevance in that the combination of several subclinical pathological alterations (eg, CNS vulnerability, immune dysregulation, induced autoimmunity) may significantly contribute to disease susceptibility or relapses.

Acknowledgments

We thank Heinrich Blazyca, Carolin Kiesel, Nadine Weckesser, Barbara Reuter, Silke Loserth, and Bettina Meyer for skilful technical assistance; and Helga Brünner and Karlheinz Aulenbach for excellent animal care.

References

1. Frohman EM, Racke MK, Raine CS: Multiple sclerosis—the plaque and its pathogenesis. N Engl J Med 2006, 354:942–955
2. Wekerle H, Kojima K, Lannes-Vieira J, Lassmann H, Linington C: Animal models. Ann Neurol 1994, 36:S47–S53
3. Steinman L: Assessment of animal models for MS and demyelinating disease in the design of rational therapy. Neuron 1999, 24:511–514
4. Bettelli E, Carrier Y, Gao W, Korn T, Strom TB, Oukka M, Weiner HL, Kuchroo VK: Reciprocal developmental pathways for the generation of pathogenic effector TH17 and regulatory T cells. Nature 2006, 441:235–238
5. Komiyama Y, Nakae S, Matsuki T, Nambu A, Ishigame H, Kakuta S, Sudo K, Iwakura Y: IL-17 plays an important role in the development of experimental autoimmune encephalomyelitis. J Immunol 2006, 177:566–573
6. Lucchinetti C, Bruck W, Parisi J, Scheithauer B, Rodriguez M, Lassmann H: Heterogeneity of multiple sclerosis lesions: implications for the pathogenesis of demyelination. Ann Neurol 2000, 47:707–717
7. Barnett MH, Prineas JW: Relapsing and remitting multiple sclerosis: pathology of the newly forming lesion. Ann Neurol 2004, 55:458–468
8. Warshawsky I, Rudick RA, Staugaitis SM, Natowicz MR: Primary progressive multiple sclerosis as a phenotype of a PLP1 gene mutation. Ann Neurol 2005, 58:470–473
9. Gorman MP, Golomb MR, Walsh LE, Hobson GM, Garbern JY, Kinkel RP, Darras BT, Urion DK, Eksioglu YZ: Steroid-responsive neurologic relapses in a child with a proteolipid protein-1 mutation. Neurology 2007, 68:1305–1307
10. Readhead C, Schneider A, Griffiths I, Nave KA: Premature arrest of myelin formation in transgenic mice with increased proteolipid protein gene dosage. Neuron 1994, 12:583–595
11. Ip CW, Kroner A, Bendszus M, Leder C, Kobsar I, Fischer S, Wiendl H, Nave KA, Martini R: Immune cells contribute to myelin degeneration and axonopathic changes in mice overexpressing proteolipid protein in oligodendrocytes. J Neurosci 2006, 26:8206–8216
12. Leder C, Schwab N, Ip CW, Kroner A, Nave KA, Dornmair K, Martini R, Wiendl H: Clonal expansions of pathogenic CD8+ effector cells in the CNS of myelin mutant mice. Mol Cell Neurosci 2007, 36:416–424
13. Keir ME, Butte MJ, Freeman GJ, Sharpe AH: PD-1 and its ligands in tolerance and immunity. Annu Rev Immunol 2008, 26:677–704
14. Keir ME, Liang SC, Guleria I, Latchman YE, Qipo A, Albacker LA, Koulmanda M, Freeman GJ, Sayegh MH, Sharpe AH: Tissue expression of PD-L1 mediates peripheral T cell tolerance. J Exp Med 2006, 203:883–895
15. Grabie N, Gotsman I, DaCosta R, Pang H, Stavrakis G, Butte MJ, Keir ME, Freeman GJ, Sharpe AH, Lichtman AH: Endothelial programmed death-1 ligand 1 (PD-L1) regulates CD8+ T-cell mediated injury in the heart. Circulation 2007, 116:2062–2071
16. Dong H, Zhu G, Tamada K, Flies DB, van Deursen JM, Chen L: B7-H1 determines accumulation and deletion of intrahepatic CD8(+) T lymphocytes. Immunity 2004, 20:327–336
17. Magnus T, Schreiner B, Korn T, Jack C, Guo H, Antel J, Ifergan I, Chen L, Bischof F, Bar-Or A, Wiendl H: Microglial expression of the B7 family member B7 homolog 1 confers strong immune inhibition: implications for immune responses and autoimmunity in the CNS. J Neurosci 2005, 25:2537–2546
18. Latchman Y, Wood CR, Chernova T, Chaudhary D, Borde M, Chernova I, Iwai Y, Long AJ, Brown JA, Nunes R, Greenfield EA, Bourque K, Boussiotis VA, Carter LL, Carreno BM, Malenkovich N, Nishimura H, Okazaki T, Honjo T, Sharpe AH, Freeman GJ: PD-L2 is a second ligand for PD-1 and inhibits T cell activation. Nat Immunol 2001, 2:261–268
19. Nishimura H, Nose M, Hiai H, Minato N, Honjo T: Development of lupus-like autoimmune diseases by disruption of the PD-1 gene encoding an ITIM motif-carrying immunoreceptor. Immunity 1999, 11:141–151
20. Nishimura H, Okazaki T, Tanaka Y, Nakatani K, Hara M, Matsumori A, Sasayama S, Mizoguchi A, Hiai H, Minato N, Honjo T: Autoimmune dilated cardiomyopathy in PD-1 receptor-deficient mice. Science 2001, 291:319–322
21. Salama AD, Chitnis T, Imitola J, Ansari MJ, Akiba H, Tushima F, Azuma M, Yagita H, Sayegh MH, Khoury SJ: Critical role of the programmed death-1 (PD-1) pathway in regulation of experimental autoimmune encephalomyelitis. J Exp Med 2003, 198:71–78
22. Carter LL, Leach MW, Azoitei ML, Cui J, Pelker JW, Jussif J, Benoit S, Ireland G, Luxenberg D, Askew GR, Milarski KL, Groves C, Brown T, Carito BA, Percival K, Carreno BM, Collins M, Marusic S: PD-1/PD-L1, but not PD-1/PD-L2, interactions regulate the severity of experimental autoimmune encephalomyelitis. J Neuroimmunol 2007, 182:124–134
23. Kroner A, Schwab N, Ip CW, Sommer C, Wessig C, Wiendl H, Martini R: The co-inhibitory molecule PD-1 modulates disease severity in a model for an inherited, demyelinating neuropathy. Neurobiol Dis 2009, 33:96–103
24. Kroner A, Schwab N, Ip CW, Leder C, Nave KA, Maurer M, Wiendl H, Martini R: PD-1 regulates neural damage in oligodendroglia-induced inflammation. PLoS ONE 2009, 4:e4405
25. Fife BT, Guleria I, Gubbels Bupp M, Eagar TN, Tang Q, Bour-Jordan H, Yagita H, Azuma M, Sayegh MH, Bluestone JA: Insulin-induced remission in new-onset NOD mice is maintained by the PD-1-PD-L1 pathway. J Exp Med 2006, 203:2737–2747
26. Wang J, Yoshida T, Nakaki F, Hiai H, Okazaki T, Honjo T: Establishment of NOD-Pdcd1−/− mice as an efficient animal model of type I diabetes. Proc Natl Acad Sci USA 2005, 102:11823–11828
27. Ito T, Ueno T, Clarkson MR, Yuan X, Jurewicz MM, Yagita H, Azuma M, Sharpe AH, Auchincloss Jr H, Sayegh MH, Najafian N: Analysis of the role of negative T cell costimulatory pathways in CD4 and CD8 T cell-mediated alloimmune responses in vivo. J Immunol 2005, 174:6648–6656
28. Kroner A, Mehling M, Hemmer B, Rieckmann P, Toyka KV, Maurer M, Wiendl H: A PD-1 polymorphism is associated with disease progression in multiple sclerosis. Ann Neurol 2005, 58:50–57
29. Ortler S, Leder C, Mittelbronn M, Zozulya AL, Knolle PA, Chen L, Kroner A, Wiendl H: B7-H1 restricts neuroantigen-specific T cell responses and confines inflammatory CNS damage: implications for the lesion pathogenesis of multiple sclerosis. Eur J Immunol 2008, 38:1734–1744
30. Schreiner B, Bailey SL, Shin T, Chen L, Miller SD: PD-1 ligands expressed on myeloid-derived APC in the CNS regulate T-cell responses in EAE. Eur J Immunol 2008, 38:2706–2717
31. Nishimura H, Minato N, Nakano T, Honjo T: Immunological studies on PD-1 deficient mice: implication of PD-1 as a negative regulator for B cell responses. Int Immunol 1998, 10:1563–1572
32. Ip CW, Kroner A, Crocker PR, Nave KA, Martini R: Sialoadhesin deficiency ameliorates myelin degeneration and axonopathic changes in the CNS of PLP overexpressing mice. Neurobiol Dis 2007, 25:105–111
33. Pannetier C, Even J, Kourilsky P: T-cell repertoire diversity and clonal expansions in normal and clinical samples. Immunol Today 1995, 16:176–181
34. Begolka WS, Vanderlugt CL, Rahbe SM, Miller SD: Differential ex-

pression of inflammatory cytokines parallels progression of central nervous system pathology in two clinically distinct models of multiple sclerosis. J Immunol 1998, 161:4437–4446
35. McMahon EJ, Bailey SL, Castenada CV, Waldner H, Miller SD: Epitope spreading initiates in the CNS in two mouse models of multiple sclerosis. Nat Med 2005, 11:335–339
36. Fazilleau N, Delarasse C, Motta I, Fillatreau S, Gougeon ML, Kourilsky P, Pham-Dinh D, Kanellopoulos JM: T cell repertoire diversity is required for relapses in myelin oligodendrocyte glycoprotein-induced experimental autoimmune encephalomyelitis. J Immunol 2007, 178:4865–4875
37. Menezes JS, van den Elzen P, Thornes J, Huffman D, Droin NM, Maverakis E, Sercarz EE: A public T cell clonotype within a heterogeneous autoreactive repertoire is dominant in driving EAE. J Clin Invest 2007, 117:2176–2185
38. Bettelli E, Pagany M, Weiner HL, Linington C, Sobel RA, Kuchroo VK: Myelin oligodendrocyte glycoprotein-specific T cell receptor transgenic mice develop spontaneous autoimmune optic neuritis. J Exp Med 2003, 197:1073–1081
39. Friese MA, Fugger L: Autoreactive CD8+ T cells in multiple sclerosis: a new target for therapy? Brain 2005, 128:1747–1763
40. Lassmann H: Experimental models of multiple sclerosis. Rev Neurol (Paris) 2007, 163:651–655
41. Werner P, Pitt D, Raine CS: Multiple sclerosis: altered glutamate homeostasis in lesions correlates with oligodendrocyte and axonal damage. Ann Neurol 2001, 50:169–180